ANTIOXIDANTS & REDOX SIGNALING
Volume 12, Number 7, 2010

DOI: 10.1089/ars.2009.2883

The Neuroprotective Functions of Selenoprotein M and its Role in Cytosolic Calcium Regulation

Mariclair A. Reeves, Frederick P. Bellinger, and Marla J. Berry

Abstract

Selenoproteins contain the trace element selenium incorporated as selenocysteine, the 21st amino acid. Some members of the selenoprotein family, such as the glutathione peroxidases, have well-characterized antioxidant activity, functioning in enzymatic breakdown of hydroperoxides to protect cells against oxidative stress. However, the functions of many of the 25 human selenoproteins, including the brain-enriched selenoprotein M, are unknown. We investigated selenoprotein M function by manipulating expression in murine hippocampal HT22 cells, cerebellar astrocyte C8-D1A cells, and primary neuronal cultures. Overexpression of the protein resulted in a reduction in reactive oxygen species and apoptotic cell death in response to oxidative challenge with hydrogen peroxide. In contrast, knock-down of selenoprotein M using shRNA in primary neuronal cultures caused apoptotic cell death comparable to levels resulting from addition of hydrogen peroxide. Calcium measurements with the indicator cameleon demonstrated that overexpression of selenoprotein M decreased calcium influx in response to hydrogen peroxide. Additionally, knock-down of selenoprotein M expression in cortical cultures caused higher baseline levels of cytosolic calcium than in control cells. These results suggest that selenoprotein M may have an important role in protecting against oxidative damage in the brain and may potentially function in calcium regulation. *Antioxid. Redox Signal.* 12, 809–818.

Introduction

Selenoproteins are defined by incorporation of selenium (Se) into the amino acid selenocysteine. This family includes twenty-five selenoproteins in humans and twenty-four in mice (25). Selenium is an essential trace element for humans and animals, as indicated by the detrimental consequences of dietary selenium deficiency seen in regions of China and New Zealand, and further highlighted by the embryonic lethality in mice resulting from targeted distribution of the tRNA required for selenocysteine incorporation (7, 34). Symptoms of Se deficiency observed in humans include Keshan disease, a potentially fatal cardiomyopathy, Kashin–Beck disease, an osteoarthropathy occurring in regions of Tibet and China where selenium is deficient, and myxedematous endemic cretinism, a form of mental retardation occurring in selenium and iodine deficient regions of Africa (6, 14). In livestock, selenium deficiency leads to reduced weight gain, diarrhea, stillbirths, diminished fertility, and white muscle disease, a disease that affects both cardiac and skeletal muscle. Moreover, accumulating evidence implicates roles for Se in physiological and pathophysiological processes, including immune function, neurodegeneration, male reproduction, and cancer incidence (6, 23, 34).

The antioxidant defense system is associated with Se. Oxidative stress is implicated in the pathogenesis of neurodegenerative diseases, such as Alzheimer's disease and Parkinson's disease (9, 16, 32). Selenoproteins with known functions include the glutathione peroxidase family (GPx), thioredoxin reductases (TRxR), and the deiodinases (DIO) (17). GPxs reduce hydrogen peroxide and alkyl hydroperoxides at the expense of glutathione, contributing to the enzymatic antioxidant defense system in mammalian cells (8, 29). The TRxR family utilizes NADPH to reduce oxidized TRxR, which is used for regenerating cellular antioxidant systems, activating signaling molecules, reducing ribonucleotides to deoxyribonucleotides for DNA synthesis, and regulating activity of transcription factors (2, 18, 30). Deiodinases convert thyroid prohormones to active hormone, and active hormones to inactive metabolites, thus regulating hormonal activity (3, 5). In addition to these characterized families, numerous selenoproteins have been identified whose functions are not known, including a family with a common redox motif. This motif consists of CXXU, where U designates selenocysteine, and it has been identified in a subset of selenoproteins, including selenoprotein M (SelM), selenoprotein 15 (Sep15), selenoprotein W (SelW), and selenoprotein T (SelT) (13, 19).

Department of Cell and Molecular Biology, John A. Burns School of Medicine, University of Hawai'i, Honolulu, Hawai'i.

Selenium is better retained in the brain than most other organs under conditions of dietary Se deficiency (4, 31). SelM is present at its highest levels in the brain (17). SelM has an endoplasmic reticulum localization signal and is retained there (17). Furthermore, changes in SelM levels were found to correlate with a mouse model for Alzheimer's disease that overexpresses a mutated form of human presenilin-2 (21). This mutation causes a form of early-onset Alzheimer's disease (24). Although the role of presenilin-2 is unclear, it is believed to regulate processing of the amyloid precursor protein, and the mutation is thought to cause buildup of a toxic fragment of amyloid beta. Mice overexpressing this mutant presenilin are deficient in SelM levels in the brain. This deficiency can be recovered by supplementing the mouse diet with sodium selenite (21).

We investigated a possible neuroprotective role of SelM in hippocampal and cerebellar astrocyte cell lines, as well as primary neuronal cultures. Because of the presence of the CXXU redox motif, we sought to determine the antioxidant properties and the potential role of SelM in protecting from oxidative stress-induced apoptosis (25). Additionally, because of the predicted location of SelM in the endoplasmic reticulum and recent studies indicating that another ER-localized selenoprotein, selenoprotein N, is required for ryanodine receptor calcium release channel activity in muscle (1, 12). We hypothesized that SelM could play a role in regulating calcium release from ER calcium stores (37).

Materials and Methods

Cell cultures

Murine HT22 hippocampal cells (obtained from R.R. Ratan, Department of Neurology, Harvard Medical School, The Beth Israel-Deaconess Medical Center) and C8-D1A cerebellar cells (American Type Culture Collection, Manassas, VA) were maintained in Dulbecco's modified Eagle's medium (Invitrogen Corp., Carlsbad, CA) containing 10% fetal bovine serum (FBS) (Invitrogen Corp.) at 5% CO_2, and 5.0% relative humidity. FBS lots were tested for Se content (Bodycote, Santa Fe Springs, CA), and the selenium concentration of media containing 10% FBS was 105 n*M*, calculated using inductively coupled plasma-mass spectrometry. For primary cultures, glass bottom tissue culture plates (World Precision Instruments, Sarasota, Fl) were coated with 0.1 mg/ml laminin in 0.1 mg/ml poly-L-lysine solution for 1 h, and then rinsed with PBS. Primary cortical cells were harvested from one day postnatal C57BL/6 mice and plated on coated dishes, and maintained in Neurobasal-A medium (Invitrogen Corp.) with 5% FBS with the addition of 100 μM glutamate (Invitrogen Corp.) to reduce glial cell growth, and enrich neuronal growth. B27 supplement (Invitrogen Corp.) was added to replace FBS after 24 h, and glutamate omitted from the media after 3 days. B27 was tested for Se content (Bodycote), and the selenium concentration of media containing 2% B27 was 93.8 n*M*, as determined by inductively coupled plasma-mass spectrometry.

Manipulation of SelM expression

A full-length human SelM cDNA (Invitrogen Corp.) was subcloned into pMSCVpuro retroviral vector (BD Biosciences Clontech, Mountain View, CA). RetroPack PT67 packaging cells (BD Biosciences Clontech) were transfected with SelM-MSCV retroviral vector or empty MSCV vector with Lipofectamine 2000 transfection reagent (Invitrogen Corp.). Transfected PT67 cells were selected in puromycin (Sigma Aldrich Co., St. Louis, MO) with the concentration of puromycin optimized (1–2 μg/ml) to kill the nontransfected control PT67 cells in 7–10 days. Transfected PT67 produced virus for viral infection of target HT22 and C8-D1A cells. HT22 and C8-D1A cells were selected with puromycin starting 48 h after viral transfection for a duration of ~7–10 days. Constructs containing short hairpin RNAs (shRNA) (Thermo Scientific, Huntsville, AL) for mouse SelM and nontarget control were subcloned into the pTRIPZ vector containing the Tet-On® inducible system with RFP. HT22 cells at 80%–90% optical confluency, or primary neuronal cultures (21 divisions) were transiently transfected with pTRIPZ vector containing nontarget shRNA control or mSelM shRNA using Lipofectamine 2000. Cells were induced with doxycycline (Clontech Laboratories, Inc.) 24 h post-transfection and incubated for 72–96 h prior to experimentation.

Reverse transcription real time PCR

RNA was harvested using an RNeasy mini kit according to the manufacture's instructions (Qiagen Inc., Valencia, CA). Synthesis of cDNA by High Capacity cDNA Reverse Transcription Kit was carried out according to manufacture's instructions (Applied Biosystems, Foster City, CA). Sequences of forward and reverse primers for real time PCR of the housekeeping gene hypoxanthine phosphoribosyl-transferase (mHPRT) (HPRT 5′: TCCTCCTCAGACCGCTTTT; HPRT 3′: CCTGGTTCATCATCGCTAATC), 18S RNA (18S 5′: CGATTG GATGGTTAGTGAGG; 18S 3′: AGTTCGACCGTCTTCTCA GC), and for SelM (SelM 5′: TGACAGTTGAATCGCCTAAA GGAG; SelM 3′: AACAGCACGAGTTCGGGGTC) are provided. Amplification of cDNA was carried out using Platinum SYBR green kits (Invitrogen Corp.) followed by detection using a 480 real time PCR machine (Roche Applied Science, Indianapolis, IN).

Radioactive ^{75}Se labeling of SelM

HT22 control and hSelM overexpressing cells were labeled by the addition of neutralized [^{75}Se] selenious acid (3 μCi/ml; specific activity, 1000 Ci/mmol), followed by incubation for 20 h. Cells were lysed with CelLytic MT (Sigma Aldrich Co., St. Louis, MO) according to the manufacturer's instructions. The proteins were separated on a 10%–20% gradient Tris-HCl Criterion Precast gel (Bio-Rad Laboratories, Inc., Hercules, CA) and transferred to polyvinylidene difluoride (PVDF). Radioactivity was detected by exposure to a phosphor screen that was subsequently imaged with a Typhoon-scanner (GE Healthcare, Piscataway, NJ).

Flow cytometry

HT22 control and hSelM overexpressing cells were plated to ~90% confluency, and subsequently challenged with 0.5 m*M*, 1.0 m*M*, and 2.0 m*M* H_2O_2 for 2 h. Following peroxide challenge, cells were incubated in dihydrorhodamine 123 (DHR1,2,3) (Invitrogen Corp.) at 37°C. The cells were rinsed with PBS, dissociated from plates with trypsin/EDTA (Invitrogen Corp.), and resuspended in PBS with 2% FBS. Mea-

surements of ROS production were carried out using flow cytometry on a FACS Caliber System (Becton Dickenson). HT22 control and shRNA SelM knock-down cells were treated in a similar fashion to overexpressing cells, except that dichlorodihydrofluorescein diacetate (H_2DCFDA) (Invitrogen Corp.), a green ROS indicator, was used due to the RFP marker in shRNA cells.

Calcium imaging

The Premo Cameleon Calcium Sensor Kit (Invitrogen Corp.) was used to transfect HT22 control and SelM overexpressing stable cell lines and primary neuronal cultures, according to manufacturer's instructions. The protein calcium indicator cameleon is a ratiometric sensor for the measurement of calcium signals with the employment of fluorescent or Förster resonance energy transfer (FRET) technology (26). The cameleon protein contains cyan fluorescent protein (CFP) and yellow fluorescent protein (YFP) modules linked with a calmodulin calcium-binding domain. The binding of calcium by the calmodulin domain causes a conformational change bringing the CFP and YFP domains in close proximity, allowing FRET to occur between the fluorophores. Excitation of CFP at 440 nm normally produces emitted light at ~460–500 nm. After binding of calcium, this energy is transferred to YFP, shifting emission to 525–560 nm. Intracellular calcium was monitored with time lapse images of cells using an Olympus IX81 spinning-disk confocal microscope (Center Valley, CA) with an environmental chamber maintained at 37°C and ~5% CO_2. The cameleon protein was excited at 440 nm, and emitted light was split into 485 nm (CFP) and 540 nm (YFP) with a Dual-View wavelength splitter (Optical Insights LLC, Santa Fe, NM). The ratio of 540 nm to 485 nm emission was used to determine internal calcium concentrations. In preliminary studies, cameleon-transfected cells were permeablized with ionomycin (Sigma Aldrich Co.) and

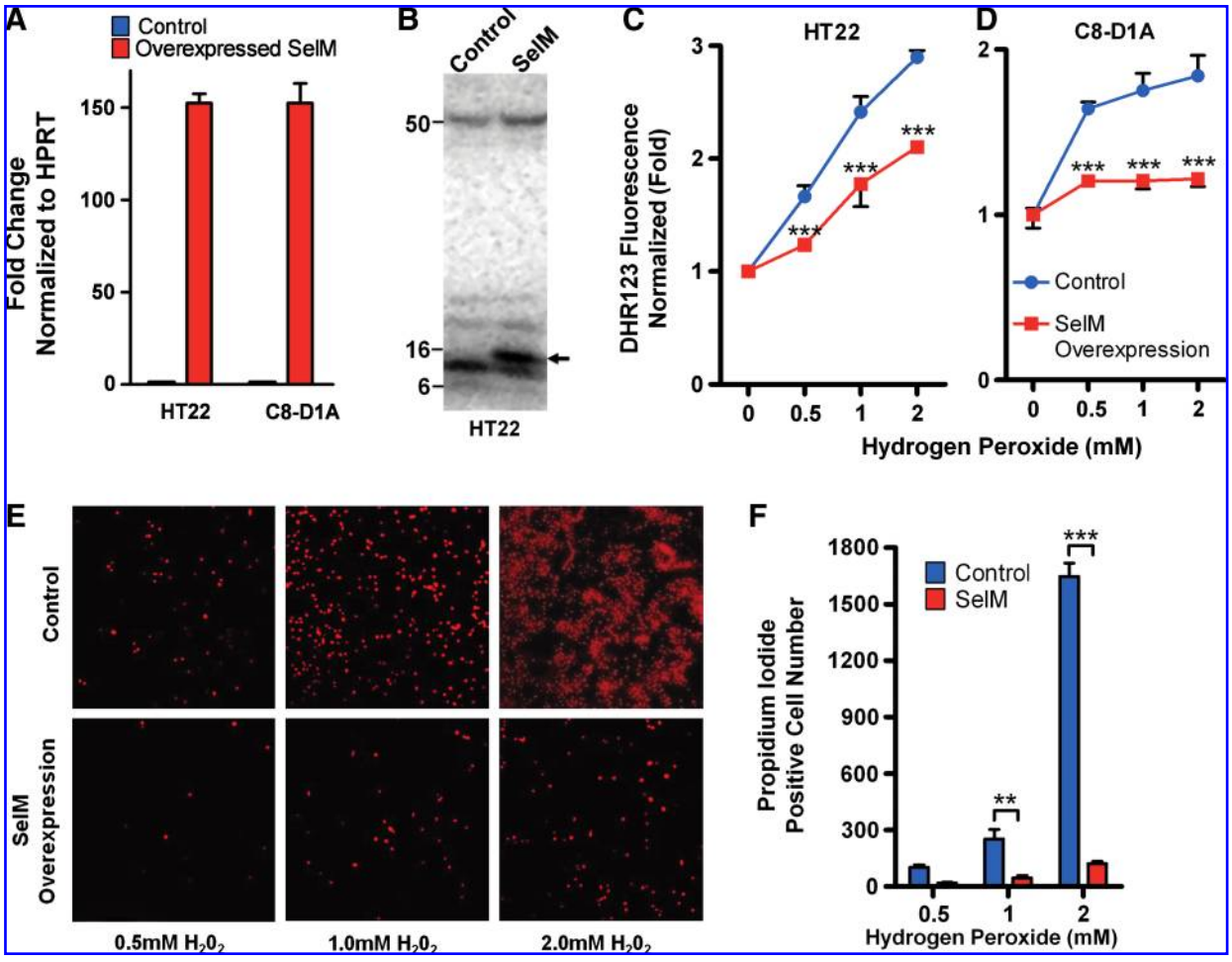

FIG. 1. SelM overexpression in HT22 cells prevented H_2O_2-induced cell death. (**A**) Quantification of SelM mRNA overexpression, relative to HPRT, using RT-PCR in mouse hippocampal HT22 cells and cerebellar astrocyte C8-D1A cells. (**B**) SelM protein overexpression in HT22 control and hSelM overexpressing cells labeled with ^{75}Se (3 μCi/ml; specific activity, 1000 Ci/mmol). (**C, D**) SelM overexpression in HT22 and C8-D1A cells decreased superoxide production, as measured with flow cytometry using DHR123. Cells were exposed to increasing concentrations of H_2O_2 (0 m*M*, 0.5 m*M*, 1.0 m*M*, and 2.0 m*M*) for 2 h, as compared to MSCV empty vector controls (***$p < 0.001$). (**E**) HT22-MSCV empty vector control and HT22-SelM overexpression cells were plated equally and then challenged with H_2O_2 (0.5 m*M*, 1.0 m*M*, 2.0 m*M*) for 4 h, and then imaged for uptake of propidium iodide to detect cells with compromised membranes. (**F**) Quantification of propidium iodide positive cells from the images in (**E**) (**$p < 0.01$; ***$p < 0.001$). (For interpretation of the references to color in this figure legend, the reader is referred to the web version of this article at www.liebertonline.com/ars).

imaged in the presence of varying external calcium concentrations. A baseline of calcium with a ratio of ~4 in HT22 and ~2 in primary cortical cells corresponds to ~100 n*M* calcium.

Cell viability

HT22 control and SelM overexpressing cells were plated to ~90% confluency and incubated with 0.5 m*M*, 1.0 m*M*, or 2.0 m*M* H_2O_2 for 4 h. Following peroxide challenge, propidium iodide (Invitrogen Corp.) was used to determine cell death, and was added to the cells in complete medium for 30 min. Images were acquired and quantified. HT22 nontarget shRNA control and SelM shRNA cells were plated at 10,000 cells per well in a 96-well format. CellTiter 96® AQ_{ueous} Non-Radioactive Cell Proliferation Assay, (MTS) assay was used to determine cell proliferation and viability according to kit instructions (Promega Corporation, Madison, WI).

Statistical analysis

Statistical comparisons were carried out using Student's *t*-test and analysis of variance (ANOVA) with Bonferroni's posthoc test for multiple comparisons. Differences were judged statistically significant at $p < 0.05$.

Results

Previous studies have shown that SelM is highly expressed in the mouse brain, with the mRNA levels present in relatively moderate amounts (37). We investigated the expression profiles of the genes for SelM and other selenoprotein family members, along with factors implicated in selenoprotein synthesis, in mouse hippocampal neuronal HT22 and mouse cerebellar astrocyte C8-D1A cell lines, and in primary mouse cortical cultures, to determine whether these cell lines are appropriate models to study SelM. SelM mRNA was present at moderate levels in all of these cell types (Supplemental Fig. 1A-C; see www.liebertonline.com/ars).

Overexpression of SelM in HT22 and C8-D1A cells protects against hydroperoxide challenge

A retroviral gene delivery system was used to overexpress SelM RNA in neuronal cells. Stable HT22 and C8-D1A cell lines showed significant overexpression of the mRNA levels for human SelM above endogenous mouse SelM mRNA (Fig. 1A). Overexpressed SelM protein was detected by ^{75}Se labeling (Fig. 1B). A band of ~15 kD, the predicted size of SelM, was clearly visible in lysates from SelM-overexpressing cells but barely detectable in control cells. The protective effects of SelM following peroxide challenge were quantified using flow cytometry. Both HT22 and C8-D1A stable overexpression cell lines were challenged using increasing concentrations of hydrogen peroxide for 2 h, and the generation of reactive oxygen species (ROS) was measured using dihydrorhodamine (DHR123) (Figs. 1C–1D). DHR123 is used as a fluorescent indicator for reactive oxygen species (ROS) generation measured such that increases in ROS production increase fluorescence (20, 33). Cells overexpressing SelM showed significantly reduced ROS production when measured by DHR123 fluorescence in the presence of varying concentrations of hydrogen peroxide (Figs. 1C–1D). Cells overexpressing SelM also exhibit increased viability compared with transfected empty vector controls following incubation with varying concentrations of hydrogen peroxide for 4 h (Fig. 1E), as shown by decreased propidium iodide (PI) fluorescence. Figure 1F indicates significantly less cell death in cells that overexpress SelM.

Knock-down of mSelM in HT22 cells and primary cortex cultures increased oxidative damage

A construct encoding short hairpin RNA (shRNA) targeted to SelM in a lentiviral expression vector with a tet-inducible promoter (pTRIPZ) was used to knock down the levels of mouse SelM mRNA to generate stable monoclonal knockdown in HT22 cells and in primary neuronal cultures. The pTRIPZ vector also contains an RFP gene for identification of transfected cells. All pTRIPZ transfected cells were induced with doxycycline from 72 to 96 h prior to experiments to ensure adequate knock-down of SelM mRNA and promote RFP activation. As additional controls, un-induced samples were tested. Four stable HT22 cell colonies were generated, and a

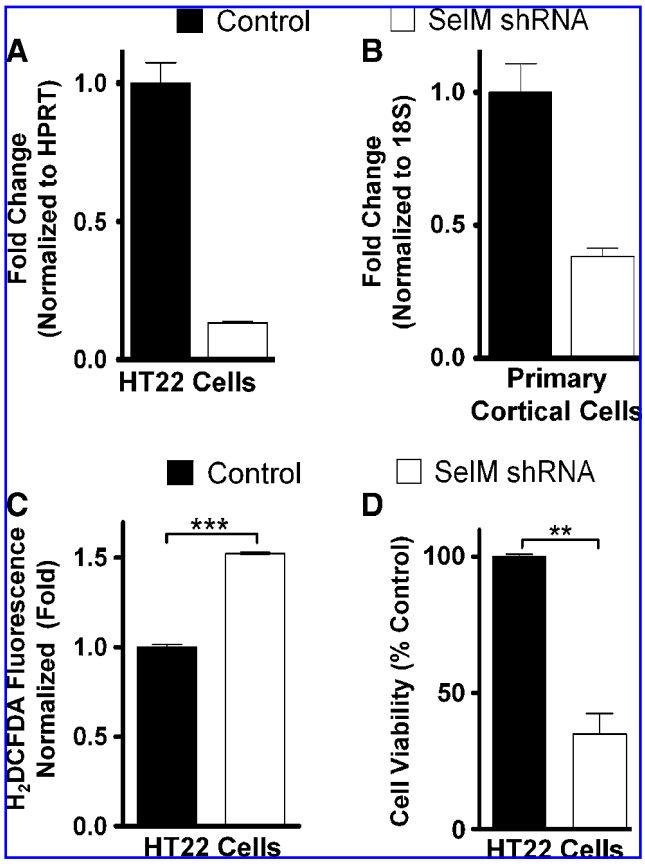

FIG. 2. Knock-down of SelM increases toxicity from oxidative stress. HT22 and primary cortical cells transfected with nontarget or SelM shRNA pTRIPZ vector and induced for 72 h. SelM mRNA levels were quantified relative to HPRT and 18S respectively using RT-PCR in (**A**) stably transfected HT22 cells and (**B**) transiently transfected primary cortical neurons. (**C**) Knock-down of SelM in HT22 cells increased reactive oxygen species as measured with H_2DCFDA and flow cytometry, as compared to nontargeting shRNA controls (***$p < 0.0001$). (**D**) Knock-down of SelM in HT22 cells decreased cell viability when measured with MTS assay, as a percent of the nontargeting shRNA control (**$p = 0.0011$).

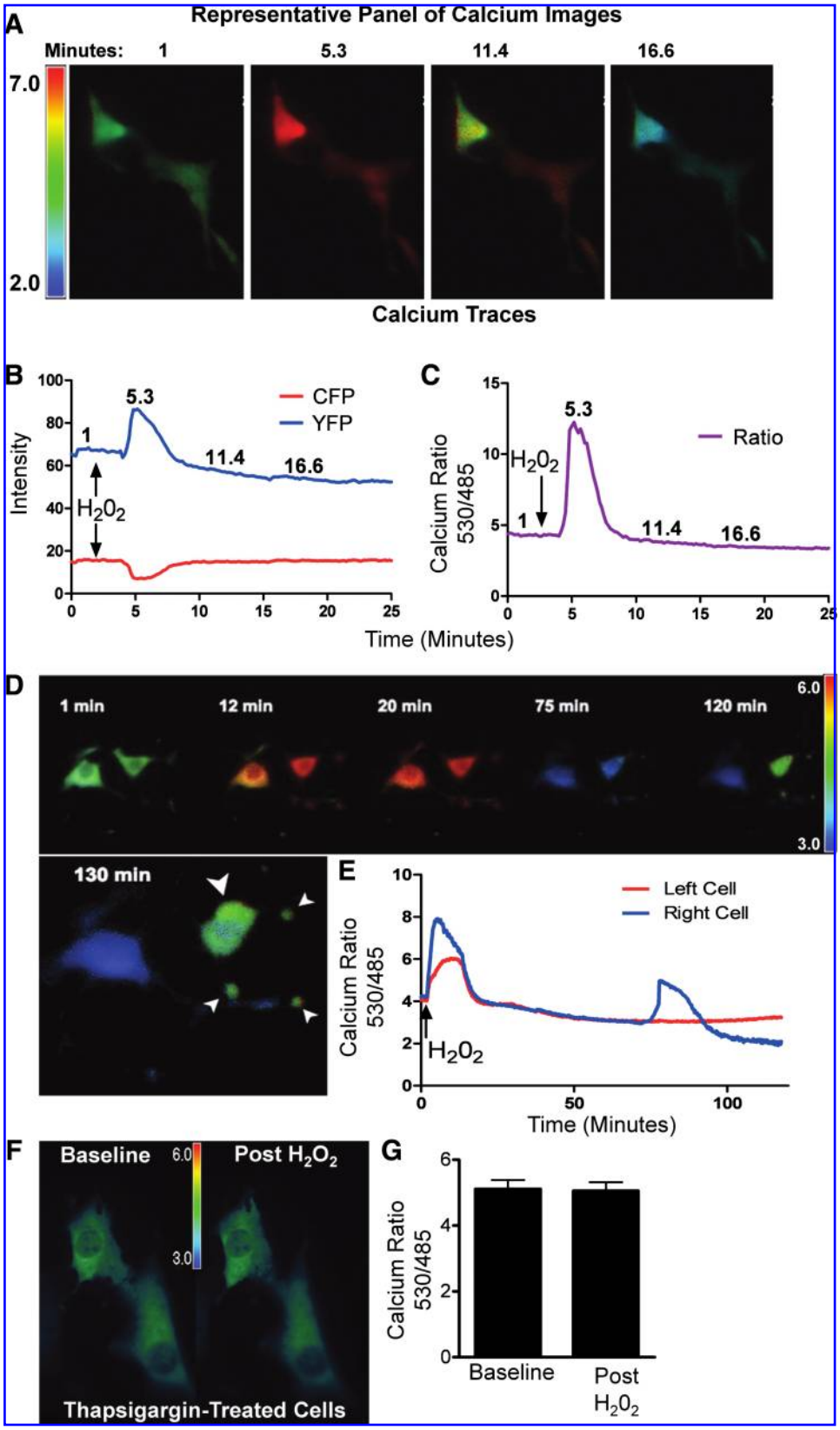

FIG. 3. Calcium responses induced by H_2O_2 in HT22 cells, measured with the cameleon protein calcium indicator. Pseudocolor changes indicate cytosolic calcium changes. (**A**) A series of representative images corresponding to (**B**) intensity of CFP and YFP and (**C**) ratio of YFP to CFP correlating with intracellular calcium levels; the numbers on the graphs **B** and **C** correspond to the images in **A**. (**D**) Examples of calcium responses to 1 m*M* H_2O_2 in two cells measured for 2 h are shown in the images in (**D**), with YFP:CFP ratio changes for the same cells graphed in (**E**). The second calcium response in the *right cell* is followed by blebbing, indicative of apoptosis (inset, *white arrows*). (**F** and **G**) Cells incubated with thapsigargin overnight showed no calcium response following addition of 1 m*M* H_2O_2, indicating that responses depend on release of calcium from intracellular stores. (For interpretation of the references to color in this figure legend, the reader is referred to the web version of this article at www.liebertonline.com/ars).

single colony exhibiting ~80% knock-down was selected for subsequent studies (Fig. 2A). Primary cells exhibited a ~60% decrease in mRNA levels compared to endogenous mRNA (Fig. 2B). ROS was also measured in knock-down cells using dichlorodihydrofluorescein diacetate (H_2DCFDA). H_2DCFDA is another indicator for ROS that is nonfluorescent until oxidation occurs within the cell to remove acetate groups (36). The stable HT22 shRNA knock-down colony was incubated with H_2DCFDA, which detected significant increases in ROS, as measured via flow cytometry (Fig. 2C). Knocking down the mRNA to ~20% of endogenous levels increased ROS even in unchallenged cells. Additionally, cell viability was measured and the results indicate a significant decrease in viable cells when knocking down SelM (Fig. 2D). The effects observed from knocking down SelM in primary cortical cells to ~40% of endogenous levels demonstrated the importance of this protein for neuronal survival.

Calcium responses induced by H_2O_2 in HT22 cells, measured with the cameleon protein calcium indicator

Having established that SelM protects against oxidative damage, and ultimately apoptosis, we hypothesized that SelM may function in regulation of calcium release from ER stores into the cytosol, due to its subcellular location within the ER, as shown in Figure 3. Cameleon was transfected into cells 48 hours prior to calcium measurements. A baseline of cytosolic calcium was initially established for each cell before oxidative challenge. Pseudocolor ratiometric images allowed visualization of calcium changes during each study (Fig. 3A). Representative panels of images from HT22 control cells transfected with the cameleon calcium indicator show the effect of 1 m*M* H_2O_2 on cytosolic calcium, indicated by color images (Fig. 3A). Following the addition of 1 m*M* H_2O_2, subsequent changes of fluorescent intensities of CFP to YFP were recorded (Fig. 3B). These fluorescent intensities are graphed as a ratiometric measurement of 530 nm (calcium-bound) to 485 nm (unbound) emission of cameleon protein over time in response to H_2O_2, indicating the changes in cytosolic calcium levels in the cell (Fig. 3C).

Calcium changes varied from cell to cell following addition of H_2O_2. Typically, peroxide caused an initial fast increase in cytosolic calcium levels, lasting many minutes before returning to basal values. In many cells, a second increase in calcium was observed, usually followed by visible signs of apoptosis, such as membrane blebbing. The second panel of images displays calcium increases following oxidative challenge, and subsequent calcium responses leading to apoptosis (Figs. 3D–3E). In order to determine whether calcium increases resulted from influx of extracellular calcium or release from endoplasmic reticulum calcium stores, cells were preincubated overnight prior to experiments with thapsigargin, to deplete internal stores (Fig. 3F). Thapsigargin is a tight-binding inhibitor of sarcoplasmic and/or endoplasmic reticulum calcium ATPase (SERCA) (35). Cells preincubated in thapsigargin did not respond to peroxide with increased cytosolic calcium levels (Fig. 3G). We also chelated external calcium using ethylene glycol tetraacetic acid (EGTA), which reduced but did not prevent responses to peroxide (data not shown). These data indicate that induction of calcium responses by peroxide is dependent upon intracellular stores and independent of extracellular calcium, although influx of extracel-

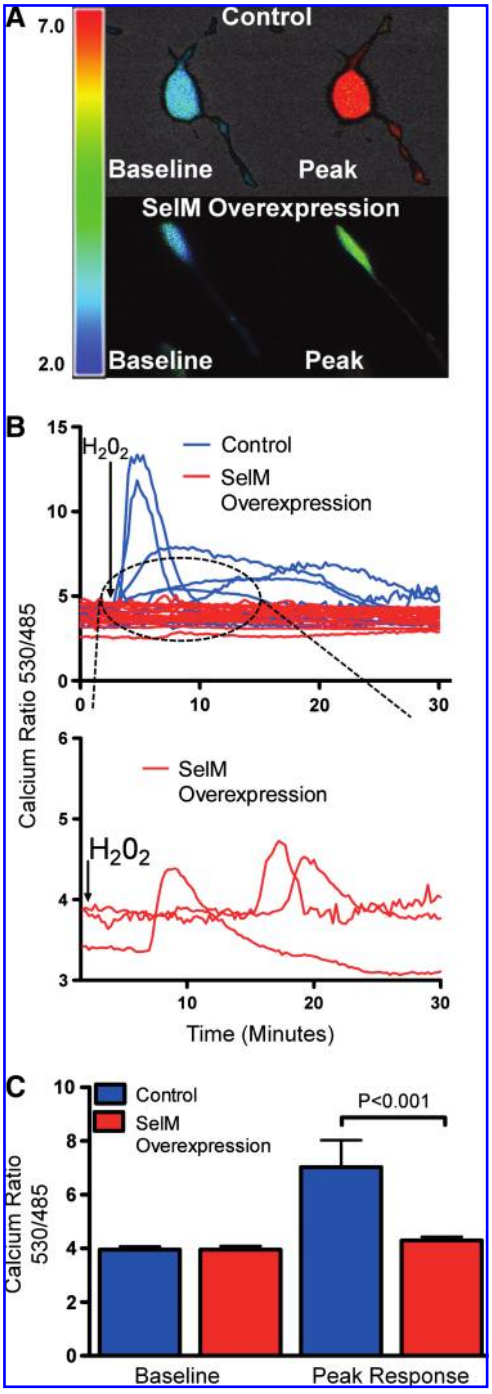

FIG. 4. SelM overexpression in HT22 cells alters cytosolic calcium responses to 1 m*M* H_2O_2. (**A**) *Top panels* are HT22 control cells, and *bottom panels* are HT22 cells overexpressing SelM; shown is baseline and following the addition of 1 m*M* H_2O_2. (**B**) Cytosolic calcium changes measured with cameleon control cells (*blue lines*, $n = 10$) and SelM overexpressing cells (*red lines*, $n = 17$). An *inset* with a subset of individual traces is shown to demonstrate the reduced calcium responses in SelM-overexpressing cells. (**C**) Baseline and peak response in HT22 control and SelM overexpression cells. Addition of H_2O_2 produced greater cytosolic calcium increases in HT22 control cells compared with SelM overexpressing cells. (For interpretation of the references to color in this figure legend, the reader is referred to the web version of this article at www.liebertonline.com/ars).

lular calcium contributes to the magnitude of subsequent responses. Thus, the initial response to peroxide is a release of calcium from intracellular stores, and is augmented by calcium influx through membrane channels.

Overexpression of SelM in HT22 cells alters cytosolic calcium in cells under oxidative stress

Having confirmed that we could accurately measure calcium changes, we examined how changes in SelM expression could alter calcium in cells under oxidative stress. Cells overexpressing SelM had smaller calcium responses compared with control cells (Fig. 4A). Responses to oxidative stress varied from cell to cell, ranging from large brief calcium increases to smaller broad responses following the addition of 1 m*M* H_2O_2 (Fig. 4B). To demonstrate the reduced calcium responses in SelM-overexpressing cells, an inset with a subset of individual traces is provided. Averaged calcium measurements from Figure 4B showed that control cells had higher levels of cytosolic calcium following the addition of hydrogen peroxide than SelM-overexpressing cells (Fig. 4C).

Knock-down of SelM in primary cortex cultures results in higher baseline cytosolic calcium levels

Individual primary cortical cultures transfected with shRNA to knock-down SelM also exhibited variable responses to oxidative stress following addition of 100 μM H_2O_2 (Fig. 5A). Calcium responses to peroxide in cortex cultures were generally much smaller than those observed in HT22

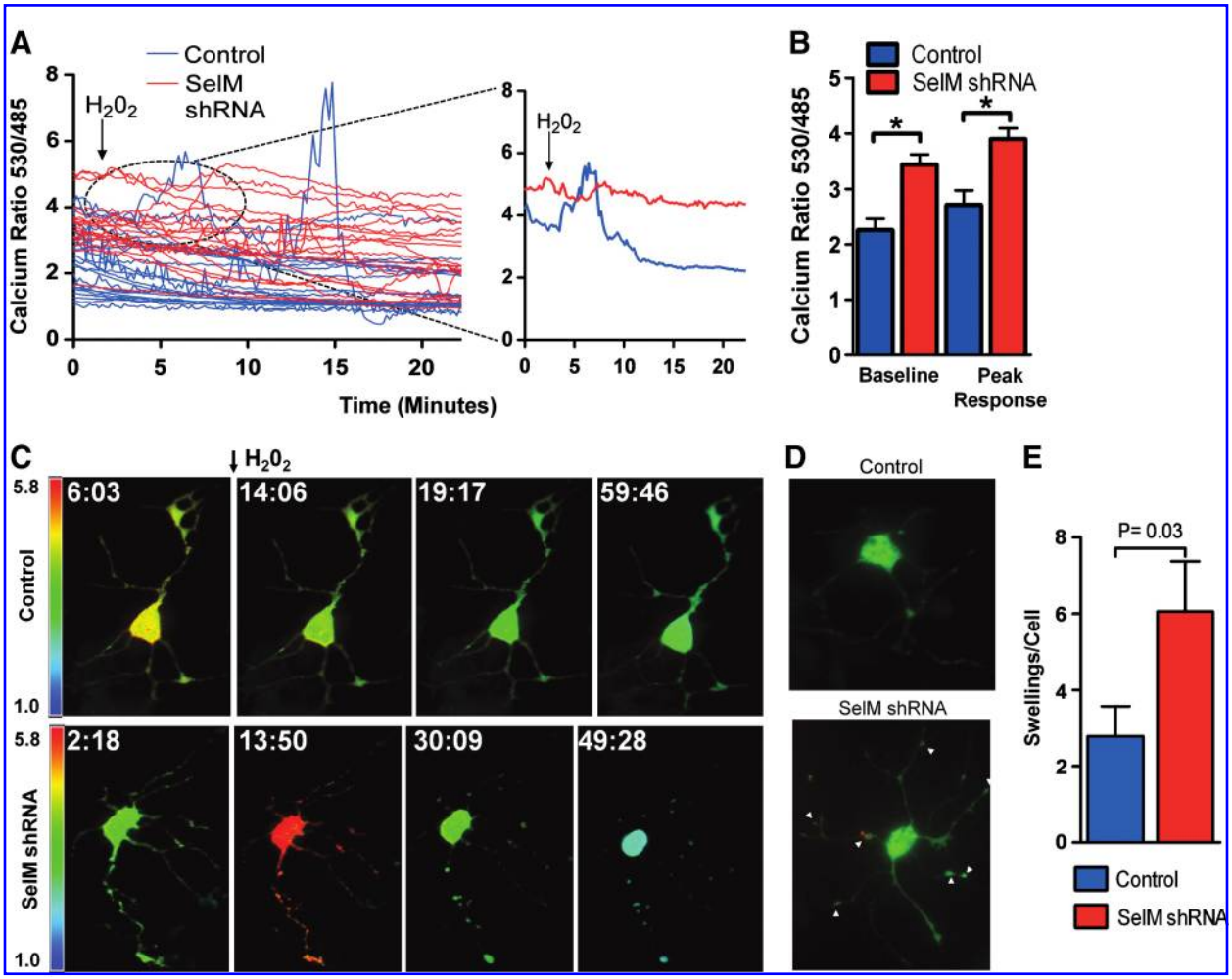

FIG. 5. Knock-down of SelM in primary cortical cells causes increased baseline calcium. (**A**) Cytosolic calcium measurements of primary cortical neurons transfected with cameleon protein in nontargeting shRNA control cells (*blue lines*, $n = 20$) and SelM shRNA-transfected cells (*red lines*, $n = 21$). The *right panel* shows two experiments demonstrating the varying calcium responses. (**B**) Average baseline calcium levels were higher in primary cortical cells transfected with SelM shRNA compared with nontargeting shRNA control cells ($^*p < 0.05$), while calcium increases in response to H_2O_2 were similar in both cells ($p > 0.05$). (**C**) A series of representative pseudocolor images of nontargeting shRNA control (*top panels*) and SelM shRNA cells (*bottom panels*) corresponding to calcium responses to 100 μM H_2O_2. (**D**) Neurons expressing SelM shRNA show blebbing in processes (indicated by *white arrows*) in response to oxidative challenge. Oxidative challenge did not cause blebbing in nontargeting shRNA controls. (**E**) An average of the number of swellings in processes observed per cell of nontargeting shRNA control cells (*blue*, $n = 14$) and SelM shRNA-transfected cells (*red*, $n = 17$) was significantly increase in SelM shRNA cells ($p = 0.03$). (For interpretation of the references to color in this figure legend, the reader is referred to the web version of this article at www.liebertonline.com/ars).

cells. Example traces showing calcium changes for knock-down SelM and control cells are provided in an inset. Averaged calcium measurements from Figure 5A shows that baseline calcium levels were increased in cells after knock-down of SelM, but the change in calcium in response to oxidative stress relative to baseline was not significantly different (Fig. 5B). Thus, these findings with primary cortical cultures are consistent with our findings in cell lines that SelM has a neuroprotective role. A series of pseudocolor images for control and SelM shRNA indicate the changes observed in cytosolic calcium (Fig. 5C). The SelM knock-down cultures often exhibit blebbing along the processes that may be indicative of apoptosis (11). Knock-down of SelM resulted in increased blebbing following peroxide-induced calcium increases, and this blebbing was not observed in control cells (Fig. 5C). Furthermore, this blebbing can be seen along the processes following knock-down of SelM prior to oxidative challenge (Fig. 5D). A quantification of the swellings along the processes, as a measure of blebbing observed in control and SelM shRNA cultures showed a significant increase in the SelM knock-down cultures compared to controls (Fig. 5E).

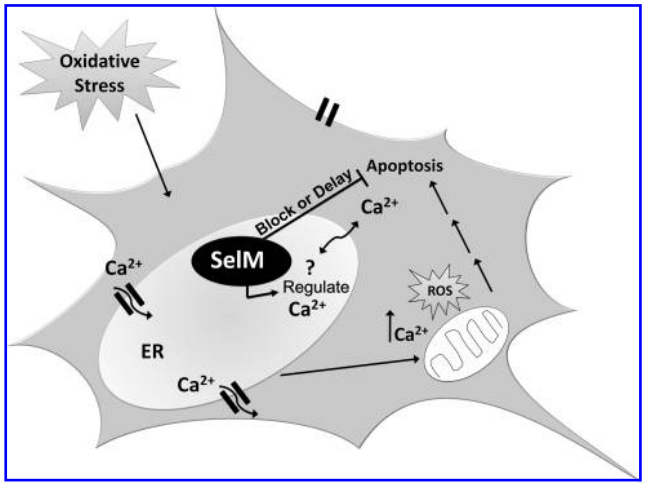

FIG. 6. Model for SelM function. SelM decreases calcium release from ER in response to oxidative stress and reduces apoptotic cell death.

Discussion

The results reported herein show that stable overexpression of SelM in HT22 hippocampal cells and C8-D1A cerebellar cells prevented oxidative damage induced by hydrogen peroxide, indicating SelM is an antioxidant protein with neuroprotective properties. As increasing SelM levels protected against oxidative stress, we hypothesized that decreasing the endogenous levels of SelM would render cells more vulnerable to oxidative challenge. Indeed, successful knock-down of SelM in HT22 cells and primary cortical cells increased oxidative damage. Furthermore, in the absence of oxidative challenge, SelM knock-down resulted in decreased cell viability and increased ROS, further demonstrating the functional importance of SelM in preventing oxidative stress. In addition, a recent study reported that overexpression of SelM in a transgenic rat model resulted in the differential regulation of antioxidants as well as the activities of antioxidant enzymes (22).

Our results show that overexpression of SelM in HT22 and C8-D1A cell lines reduced changes in cytosolic calcium evoked by oxidative stress, without affecting basal calcium levels. This indicates that SelM influences the process through which cells release calcium from their internal stores and, ultimately, may alter apoptotic pathways (10). In primary cortical cultures, knock-down of SelM increased baseline levels of calcium. Taken together, these data suggest that calcium regulation was impaired with SelM knock-down. The inability to detect significant calcium responses to oxidative stress under conditions of SelM knock-down may have been a consequence of the increased basal calcium in these cultures.

The importance of calcium regulation for neuronal viability and responses to oxidative stress is well documented, highlighting the potential importance of SelM in this capacity (27). In addition, disruption of neuronal calcium homeostasis is implicated in the mechanism of neuron degeneration in several diseases, including Alzheimer's disease and Huntington's disease (28). A diagrammatic model of the proposed antioxidant and calcium regulation functions of SelM is shown in Figure 6. Increased oxidative stress leads to increases in calcium and ROS, triggering apoptosis. Overexpression of SelM, which is localized to the endoplasmic reticulum (15), blocks or delays apoptosis. Questions still remain as to how SelM influences calcium, and whether this action is direct or indirect, and thus further investigation of this protein will be necessary to determine the pathways through which SelM functions as a neuroprotective antioxidant.

Acknowledgments

This study was supported by NIH grants DK47320 and NS40302 to MJB; Hawaii Community Foundation grant 20061490 to FPB; and NIH RR003061 and RR016467 for the JABSOM Microscopy and Imaging core facility. We thank Dr. Robert Nichols for helpful comments and suggestions, and thank Ann Hashimoto, Andrea Takemoto, and Miyoko Bellinger for technical assistance.

Author Disclosure Statement

No competing financial interests exist.

References

1. Arbogast S, Beuvin M, Fraysse B, Zhou H, Muntoni F, and Ferreiro A. Oxidative stress in SEPN1-related myopathy: From pathophysiology to treatment. *Ann Neurol* 65: 677–686, 2009.
2. Arner ES and Holmgren A. Physiological functions of thioredoxin and thioredoxin reductase [In Process Citation]. *Eur J Biochem* 267: 6102–6109, 2000.
3. Arthur JR, Nicol F, and Beckett GJ. Hepatic iodothyronine 5′-deiodinase. The role of selenium. *Biochem J* 272: 537–540, 1990.
4. Behne D, Hilmert H, Scheid S, Gessner H, and Elger W. Evidence for specific selenium target tissues and new biologically important selenoproteins. *Biochim Biophys Acta* 966: 12–21, 1988.
5. Behne D, Kyriakopoulos A, Meinhold H, and Köhrle J. Identification of type I iodothyronine 5′-deiodinase as a selenoenzyme. *Biochem Biophys Res Commun* 173: 1143–1149, 1990.

6. Bellinger FP, Raman AV, Reeves MA, and Berry MJ. Regulation and function of selenoproteins in human diseases. *Biochem J* 422: 11–22, 2009.
7. Bosl MR, Takaku K, Oshima M, Nishimura S, and Taketo MM. Early embryonic lethality caused by targeted disruption of the mouse selenocysteine tRNA gene (Trsp). *Proc Natl Acad Sci USA* 94: 5531–5534, 1997.
8. Brigelius-Flohe R. Tissue-specific functions of individual glutathione peroxidases. *Free Radic Biol Med* 27: 951–965, 1999.
9. Butterfield DA. Amyloid beta-peptide (1-42)-induced oxidative stress and neurotoxicity: Implications for neurodegeneration in Alzheimer's disease brain. A review. *Free Radic Res* 36: 1307–1313, 2002.
10. Clapham DE. Calcium signaling. *Cell* 131: 1047–1058, 2007.
11. D'Amelio M, Cavallucci V, Diamantini A, and Cecconi F. Analysis of neuronal cell death in mammals. *Methods Enzymol* 446: 259–276, 2008.
12. Deniziak M, Thisse C, Rederstorff M, Hindelang C, Thisse B, and Lescure A. Loss of selenoprotein N function causes disruption of muscle architecture in the zebrafish embryo. *Exp Cell Res* 313: 156–167, 2007.
13. Dikiy A, Novoselov SV, Fomenko DE, Sengupta A, Carlson BA, Cerny RL, Ginalski K, Grishin NV, Hatfield DL, and Gladyshev VN. SelT, SelW, SelH, and Rdx12: Genomics and molecular insights into the functions of selenoproteins of a novel thioredoxin-like family. *Biochemistry* 46: 6871–6882, 2007.
14. Dubois F and Belleville F. [Selenium: physiologic role and value in human pathology]. *Pathol Biol (Paris)* 36: 1017–1025, 1988.
15. Ferguson AD, Labunskyy VM, Fomenko DE, Araç D, Chelliah Y, Amezcua CA, Rizo J, Gladyshev VN, and Deisenhofer J. NMR structures of the selenoproteins Sep15 and SelM reveal redox activity of a new thioredoxin-like family. *J Biol Chem* 281: 3536–3543, 2006.
16. Foley P and Riederer P. Influence of neurotoxins and oxidative stress on the onset and progression of Parkinson's disease. *J Neurol* 247: II82–II94, 2000.
17. Gromer S, Eubel JK, Lee BL, and Jacob J. Human selenoproteins at a glance. *Cell Mol Life Sci* 62: 2414–2437, 2005.
18. Gromer S, Urig S, and Becker K. The thioredoxin system—From science to clinic. *Med Res Rev* 24: 40–89, 2004.
19. Hatfield DL and Gladyshev VN. How selenium has altered our understanding of the genetic code. *Mol Cell Biol* 22: 3565–3576, 2002.
20. Henderson LM and Chappell JB. Dihydrorhodamine 123: A fluorescent probe for superoxide generation? *Eur J Biochem* 217: 973–980, 1993.
21. Hwang DY, Cho JS, Oh JH, Shim SB, Jee SW, Lee SH, Seo SJ, Lee SK, Lee SH, and Kim YK. Differentially expressed genes in transgenic mice carrying human mutant presenilin-2 (N141I): Correlation of selenoprotein M with Alzheimer's disease. *Neurochem Res* 30: 1009–1019, 2005.
22. Hwang DY, Sin JS, Kim MS, Yim SY, Kim YK, Kim CK, Kim BG, Shim SB, Jee SW, Lee SH, Bae CJ, Lee BC, Jang MK, Cho JS, and Chae KR. Overexpression of human selenoprotein M differentially regulates the concentrations of antioxidants and H2O2, the activity of antioxidant enzymes, and the composition of white blood cells in a transgenic rat. *Int J Mol Med* 21: 169–179, 2008.
23. Koller LD and Exon JH. The two faces of selenium-deficiency and toxicity—Are similar in animals and man. *Can J Vet Res* 50: 297–306, 1986.
24. Kowalska A, Pruchnik-Wolińska D, Florczak J, Modestowicz R, Szczech J, Kozubski W, Rossa G, and Wender M. Genetic study of familial cases of Alzheimer's disease. *Acta Biochim Pol* 51: 245–252, 20204.
25. Kryukov GV, Castellano S, Novoselov SV, Lobanov AV, Zehtab O, Guigó R, and Gladyshev VN. Characterization of mammalian selenoproteomes. *Science* 300: 1439–1443, 2003.
26. Liu X, Gong H, Li X, and Zhou W. Monitoring calcium concentration in neurons with cameleon. *J Biosci Bioeng* 105: 106–109, 2008.
27. Mattson MP. Calcium and neurodegeneration. *Aging Cell* 6: 337–350, 2007.
28. Mattson MP. Cellular actions of beta-amyloid precursor protein and its soluble and fibrillogenic derivatives. *Physiol Rev* 77: 1081–1132, 1997.
29. Michiels C, Raes M, Toussaint O, and Remacle J. Importance of Se-glutathione peroxidase, catalase, and Cu/Zn-SOD for cell survival against oxidative stress. *Free Radic Biol Med* 17: 235–248, 1994.
30. Nakamura H. Thioredoxin and its related molecules: Update 2005. *Antioxid Redox Signal* 7: 823–828, 2005.
31. Nakayama A, Hill KE, Austin LM, Motley AK, and Burk RF. All regions of mouse brain are dependent on selenoprotein P for maintenance of selenium. *J Nutr* 137: 690–693, 2007.
32. Przedborski S, Mitsumoto H, and Rowland LP. Recent advances in amyotrophic lateral sclerosis research. *Curr Neurol Neurosci Rep* 3: 70–77, 2003.
33. Qian Y, Banerjee S, Grossman CE, Amidon W, Nagy G, Barcza M, Niland B, Karp DR, Middleton FA, Banki K, and Perl A. Transaldolase deficiency influences the pentose phosphate pathway, mitochondrial homoeostasis and apoptosis signal processing. *Biochem J* 415: 123–134, 2008.
34. Rayman MP. The importance of selenium to human health. *Lancet* 356: 233–241, 2000.
35. Rogers TB, Inesi G, Wade R, and Lederer WJ. Use of thapsigargin to study Ca2+ homeostasis in cardiac cells. *Biosci Rep* 15: 341–349, 1995.
36. Wardman P. Methods to measure the reactivity of peroxynitrite-derived oxidants toward reduced fluoresceins and rhodamines. *Methods Enzymol* 441: 261–282, 2008.
37. Zhang Y, Zhou Y, Schweizer u, Savaskan NE, Hua D, Kipnis J, Hatfield DL, and Gladyhev VN. Comparative analysis of selenocysteine machinery and selenoproteome gene expression in mouse brain identifies neurons as key functional sites of selenium in mammals. *J Biol Chem* 283: 2427–2438, 2008.

Address correspondence to:
Mariclair Reeves
Cell and Molecular Biology Department
University of Hawai'i
651 Ilalo Street
Honolulu, HI 96813

E-mail: marci.reeves@gmail.com

Date of first submission to ARS Central, September 8, 2009; date of acceptance, September 19, 2009.

Abbreviations Used

CFP = cyan fluorescent protein
DHR123 = dihydrorhodamine
EGTA = glycol tetraacetic acid
ER = endoplasmic reticulum
FRET = fluorescent or Förster resonance energy transfer
GPx = glutathione peroxidase
GSH = glutathione
H_2DCFDA = dichlorodihydrofluorescein diacetate
H_2O_2 = hydrogen peroxide
HPRT = hypoxanthine-guanine phosphoribosyltransferase
MTS = tetrazolium compound: [3-(4,5-dimethylthiazol-2-yl)-5-(3-carboxymethoxyphenyl)-2-(4-sulfophenyl)-2H-tetrazolium, inner salt
PI = propidium iodide
ROS = reactive oxygen species
RT-PCR = reverse-transcriptase real-time PCR
Se = selenium
SelM = selenoprotein M
shRNA = short-hairpin RNA
TRxR = thioredoxin reductase
TUNEL = Terminal deoxynucleotidyl Transferase dUTP Nick End Labeling
U = selenocysteine
YFP = yellow fluorescent protein

This article has been cited by:

1. Marina V. Kasaikina, Dolph L. Hatfield, Vadim N. Gladyshev. 2012. Understanding selenoprotein function and regulation through the use of rodent models. *Biochimica et Biophysica Acta (BBA) - Molecular Cell Research* **1823**:9, 1633-1642. [CrossRef]
2. Stéphane Tanguy, Stéphane Grauzam, Joël de Leiris, François Boucher. 2012. Impact of dietary selenium intake on cardiac health: Experimental approaches and human studies. *Molecular Nutrition & Food Research* **56**:7, 1106-1121. [CrossRef]
3. C. Meplan, J. Hesketh. 2012. The influence of selenium and selenoprotein gene variants on colorectal cancer risk. *Mutagenesis* **27**:2, 177-186. [CrossRef]
4. Arjun V. Raman, Marla J. BerrySelenoproteins in Cellular Redox Regulation and Signaling 195-208. [CrossRef]
5. Ji-Chang Zhou, Hua Zhao, Jia-Yong Tang, Jun-Gang Li, Xiao-Li Liu, Yu-Mei Zhu. 2011. Molecular cloning, chromosomal localization and expression profiling of porcine selenoprotein M gene. *Genes & Genomics* **33**:5, 529-534. [CrossRef]
6. Ohad S Birk. 2011. Selenocysteinopathies: progressive cerebello–cerebral atrophy and other diseases of the 21st amino acid, selenocysteine. *Future Neurology* **6**:2, 135-138. [CrossRef]
7. Catherine Méplan. 2011. Trace elements and ageing, a genomic perspective using selenium as an example. *Journal of Trace Elements in Medicine and Biology* **25**, S11-S16. [CrossRef]
8. Laura V. Papp , Arne Holmgren , Kum Kum Khanna . 2010. Selenium and Selenoproteins in Health and Disease. *Antioxidants & Redox Signaling* **12**:7, 793-795. [Abstract] [Full Text HTML] [Full Text PDF] [Full Text PDF with Links]